Forensic Science International 264 (2016) 63–69

Contents lists available at ScienceDirect

Forensic Science International

journal homepage: www.elsevier.com/locate/forsciint

Fluorescently labeled bacteria provide insight on post-mortem microbial transmigration

Z.M. Burcham [a,1], J.A. Hood [a,2], J.L. Pechal [b,3], K.L. Krausz [c,4], J.L. Bose [c,4], C.J. Schmidt [d,5], M.E. Benbow [b,e,6,7], H.R. Jordan [a,8,*]

[a] Department of Biological Sciences, Mississippi State University, Starkville, MS, USA
[b] Department of Entomology, Michigan State University, East Lansing, MI, USA
[c] Department of Microbiology, Molecular Genetics, and Immunology, University of Kansas Medical Center, Kansas City, KS, USA
[d] Department of Pathology, University of Michigan, MI, USA
[e] Department of Osteopathic Medical Specialties, Michigan State University, East Lansing, MI, USA

ARTICLE INFO

Article history:
Available online 17 March 2016

Keywords:
Forensics
Staphylococcus aureus
Clostridium perfringens
Necrobiome
Decomposition

ABSTRACT

Microbially mediated mechanisms of human decomposition begin immediately after death, and are a driving force for the conversion of a once living organism to a resource of energy and nutrients. Little is known about post-mortem microbiology in cadavers, particularly the community structure of microflora residing within the cadaver and the dynamics of these communities during decomposition. Recent work suggests these bacterial communities undergo taxa turnover and shifts in community composition throughout the post-mortem interval. In this paper we describe how the microbiome of a living host changes and transmigrates within the body after death thus linking the microbiome of a living individual to post-mortem microbiome changes. These differences in the human post-mortem from the ante-mortem microbiome have demonstrated promise as evidence in death investigations. We investigated the post-mortem structure and function dynamics of *Staphylococcus aureus* and *Clostridium perfringens* after intranasal inoculation in the animal model *Mus musculus* L. (mouse) to identify how transmigration of bacterial species can potentially aid in post-mortem interval estimations. *S. aureus* was tracked using *in vivo* and *in vitro* imaging to determine colonization routes associated with different physiological events of host decomposition, while *C. perfringens* was tracked using culture-based techniques. Samples were collected at discrete time intervals associated with various physiological events and host decomposition beginning at 1 h and ending at 60 days post-mortem. Results suggest that *S. aureus* reaches its highest concentration at 5–7 days post-mortem then begins to rapidly decrease and is undetectable by culture on day 30. The ability to track these organisms as they move in to once considered sterile space may be useful for sampling during autopsy to aid in determining post-mortem interval range estimations, cause of death, and origins associated with the geographic location of human remains during death investigations.

* Corresponding author at: P.O. Box GY, Mississippi State, MS 39762, USA. Tel.: +1 662 325 8252.
E-mail addresses: zmb50@msstate.edu (Z.M. Burcham), jah842@msstate.edu (J.A. Hood), pechalje@msu.edu (J.L. Pechal), kkrausz@kumc.edu (K.L. Krausz), jbose@kumc.edu (J.L. Bose), cjschmidt@earthlink.net (C.J. Schmidt), benbow@msu.edu (M.E. Benbow), jordan@biology.msstate.edu (H.R. Jordan).
[1] Address: Department of Biology, Mississippi State University, 20 Harned Hall, 295 Lee Boulevard, Mississippi State, MS 37962, USA. Tel.: +1 865 640 4889.
[2] Address: Department of Biology, Mississippi State University, 295 Lee Boulevard, Mississippi State, MS 37962, USA.
[3] Address: Department of Entomology, Michigan State University, 243 Natural Science Building, East Lansing, MI 48824, USA. Tel.: +1 517 355 6514.
[4] Address: Department of Microbiology, Molecular Genetics & Immunology, University of Kansas Medical Center, USA.
[5] Address: Department of Pathology, University of Michigan, Wayne County, MI, USA. Tel.: +1 313 833 2504.
[6] Address: Department of Entomology, Michigan State University, 243 Natural Science Building, 288 Farm Lane Road, East Lansing, MI 48824, USA. Tel.: +1 517 229 2540.
[7] Address: Department of Osteopathic Medicine, Michigan State University, 243 Natural Science Building, 288 Farm Lane Road, East Lansing, MI 48824, USA. Tel.: +1 517 229 2540.
[8] Address: Department of Biology, Mississippi State University, 219 Harned Hall, 295 Lee Boulevard, Mississippi State, MS 37962, USA. Tel.: +1 865 804 4920.

http://dx.doi.org/10.1016/j.forsciint.2016.03.019

1. Introduction

Identification of a biological indicator that is consistently identified on cadavers and exhibits similar post-mortem patterns regardless of the death circumstances could be crucial in narrowing a post-mortem interval (PMI) range estimate. Only a few studies have focused on commensal microbial communities (*i.e.*, located internally and externally of a living person) for determining dynamics, such as microbial transmigration, under carefully controlled conditions following host death [1–4]. Here we present a controlled study used to determine the bacterial movement of intentionally infected model organisms from a specific anatomical location during the progression of host decomposition. We co-infected mice nasally with *Clostridium perfringens* and a *Staphylococcus aureus* strain with constitutively expressed fluorescent protein. *S. aureus* is a facultative anaerobe of the phylum Firmicutes, and is a natural commensal of the nares [5]. *C. perfringens* is a strict anaerobe and normal commensal of the gastrointestinal tract [6,7]. Both of these bacterial species were previously found associated with the decomposition of human surrogates [3,8,9]. We tracked these bacteria using *in vivo* and *in vitro* imaging and/or culture in order to determine colonization routes associated with bacterial oxygen requirements, anatomical location, and different physiological events of host decomposition. Additionally, a subset of mice was immediately surface sterilized following sacrifice and compared to non-surface sterilized in order to determine the influence of external microbiota on colonization.

2. Materials and methods

2.1. Construction of S. aureus KUB7

To construct a *S. aureus* strain with constitutively expressed fluorescent protein, the gene encoding a codon-optimized DsRed.T3 (DNT) was amplified by PCR from pRFP-F (Table 1) [10] using primers JBKU13 and JBKU14. This construct also contains an optimized ribosome binding site for enhanced expression. The resulting PCR product was cloned downstream of the constitutively expressed P_{sarAP1} promoter in pCM29 [11] using EcoRI and KpnI, replacing the *gfp* gene in this plasmid. The resulting plasmid, pJB1005, was digested with PstI and EcoRI and the fragment containing the P_{sarAP1}::*dsRed* construct was ligated into the same sites of pJC1112 [12], resulting in pJB1008. Next, pJB1008 was transformed into strain DC10B to facilitate electroporation. pJB1008 was isolated from DC10B and used for electroporation of AH1263 containing the integration helper plasmid pRN7023, leading to integration of pJB1008 into the SaPI1 site. Integration was confirmed using primers JCO717 and JBKU13. To ensure loss of pRN7023, the integrated pJB1008 was transferred into AH1263 using Φ11-mediated phage transduction as previously described [13]. Bacterial strains and plasmids used for this study are listed in Table 2.

2.2. Molecular genetic techniques

All manipulations were performed in *Escherichia coli* DH5α. *E. coli* was grown in LB media supplemented with ampicillin (100 μg ml^{-1}) as necessary. *S. aureus* was grown in TSB with erythromycin (5 μg ml^{-1}) or chloramphenicol (10 μg ml^{-1}) as needed for selection. Solid media contained 1.5% agar. Oligonucleotides were synthesized by Integrated DNA Technologies (Coralville, IA). High-fidelity PCR for cloning purposes was performed using KOD DNA Polymerase (Novagen, Madison, WI) while chromosome integration confirmation utilized Midas Master Mix (Monserate Biotechnology Group, San Diego, CA). PCR was performed on an Applied Biosystems GeneAmp 9700 (Life Technologies) and products were purified using the DNA Clean and Concentrator-5 kit (Zymo Research, Orange, CA). Plasmids were purified with the Wizard Plus SV Minipreps DNA Purification System (Promega Corporation, Madison, WI). Restriction endonucleases and T4 DNA Ligase were purchased from New England Biolabs (Beverly, MA). All PCR products were sequenced by ACGT, Inc (Wheeling, IL) to ensure there were no unintended changes and sequencing data was analyzed using Vector NTI (ThermoFisher Scientific).

Table 1
Primers used in this study.

Name	Sequence (5′ → 3′)[a]	Reference
JBKU13	*ccggtacc*TGATTAACTTTATAAGGAGGAAAAACATATGG	This study
JBKU14	*ccgaatt*CATCTGTGGTATGGCGCTAG	This study
JCO717	GTGCTTCACCAGCACCACATGCTG	[12]

[a] Lower-case italicized bases are non-homologous nucleotides added for cloning purposes.

Table 2
Bacterial strains and plasmids used in this study and associated references.

	Characteristics[a, b]	Reference
Bacteria		
E. coli DC10B	Δ*hsdRMS* Δ*dcm*	[14]
S. aureus AH1263	CA-MRSA USA300 strain LAC without LAC-p03	[15]
S. aureus KUB7	AH1263 with pJB1008 in SaPI1 site	This study
Plasmid		
pCM29	Amp^r Chl^r Source of P_{sarAP1}	[11]
pJB1005	P_{sarAP1}::*dsRed* in pCM29	This study
pJB1008	P_{sarAP1}::*dsRed* in pJC1112	This study
pJC1112	Ery^r SaPI1 integration plasmid	[12]
pRFP-F	Source of *dsRed*	[10]
pRN7023	Chl^r Integration helper plasmid	[12]

[a] dsRed encodes DsRed.T3(DNT).
[b] Ery^r and Chl^r denote erythromycin and chloramphenicol resistance for *S. aureus*, respectively. Amp^r identifies ampicillin resistance in *E. coli*.

2.2.1. C. perfringens preparation

C. perfringens type A strain WAL 14572 was obtained from ATCC, and maintained anaerobically on reinforced clostridial medium (BD) agar at 37 °C prior to infection. *C. perfringens* was used as a negative control for aerobic nasal inoculation as this species is a strict anaerobe.

2.2.2. Inoculum preparation

S. aureus KUB7 was grown in tryptic soy broth (TSB) to an optical density (OD_{600}) of 0.5–0.55 while *C. perfringens* was grown in 100 mL of reinforced clostridial medium (RCM) broth to an OD_{600} of 0.3–0.35. One milliliter of each culture was aliquoted into a total of 64 tubes containing 1 mL of respective bacterial suspension, then centrifuged at 12,000 × *g* for 10 min to pellet the cells. Each inoculum was individually plated, then *S. aureus* KUB7 was resuspended in 7 μl of TSB and added to *C. perfringens* resuspended in 7 μl of RCM broth containing 60 g/L of sucrose. The final inoculum was 2.8×10^8 CFU/mL and 2.24×10^7 CFU/mL for *S. aureus* KUB7 and *C. perfringens*, respectively.

2.2.3. Animals

Ninety healthy female, SKH-1 Elite female mice, weighing 16–22 g and of 9–12 weeks of age, were obtained from Charles River Laboratories and included in experiments of nares infection studies. SKH-1 mice are hairless, euthymic and immunocompetent. Mice were housed at a constant room temperature (25 °C) with a natural day/night light cycle (12L:12D) in a conventional animal colony at the Mississippi State University Veterinary

School. Standard, antibiotic-free laboratory food and water was provided *ad libitum*. Before experiments, mice were adapted to conditions for a period of 5 days. Mice were equally divided among three treatment groups: (1) control, uninfected mice; (2) infected mice without post-mortem surface sterilization; and (3) infected mice with post-mortem surface sterilization. All animal experiments were conducted according to Mississippi State University IACUC approved protocol 14–102.

2.2.4. Intentional bacterial inoculation and sacrifice

Mice were sedated with isoflurane and randomly chosen and inoculated nasally (allowing the mice to inhale) with the previously described *S. aureus* KUB7/*C. perfringens* mix ($N = 60$) or were used as control, uninfected mice ($N = 30$). Mice were sorted into habitats according to their treatment of being either infected without surface sterilization post-mortem, infected with surface sterilization post-mortem, or an uninfected control. Mice were sacrificed 24 h post infection by cervical dislocation. Thirty of the inoculated mice were surface sterilized by submerging the body in a 10% bleach solution for 45 s while being careful to avoid submerging the ears, mouth, and nares. The bleached mice were then immediately rinsed twice with distilled water. The remaining 30 inoculated mice were not surface sterilized. All mice were placed individually in to a Nalgene bottle top 0.2 μm filter container (Thermo Scientific) sealed with Parafilm M and placed in a room of ambient temperature within a bilaminar flow hood with continuous airflow.

2.2.5. Dissection and organ harvest

Three mice per treatment were analyzed per time point ($T = 1H$, 3H, 5H, 24H, 5D, 7D, 14D, 30D, and 60D post-mortem). Mouse skin was swabbed as a composite using a sterile cotton swab saturated in nuclease free water and by swabbing both dorsal and ventral sides; the swab was immediately swabbed on to a mannitol salt agar (MSA) and RCM plate and then transferred into a 2.0 mL screwcap tube to be frozen for future companion studies. The initial incision took place vertically from the lower throat to above the genitalia using sterile blades for each mouse. The liver, lungs, spleen, heart, stomach, one kidney, and a composite of the intestines were extracted using individual, sterile forceps and placed into respective 2.0 mL screw cap tube. Each organ was crushed with a sterile cotton swab and swabbed on to a MSA and RCM plate. Afterwards, the preservation solution RNA*later*® (Ambion) was added to each organ tube. The MSA plates were incubated 1–2 days aerobically at 37 °C and the RCM plates were incubated 1 day anaerobically at 37 °C. Plates were visualized for signs of growth.

2.2.6. Plate analysis

Isolates from the RCM plates for each organ were counted and recorded. Colony counts greater than or equal to 300 colonies on a single plate were recorded as "maximum countable colonies"; MSA plates were counted and recorded prior to assessment of red fluorescence. The MSA plates containing growth were analyzed for the number of red fluorescence colonies compared to the total number of colonies to obtain a percent of fluorescent colonies. Fluorescent analysis was performed using an EVOS digital inverted microscope (AMG).

2.2.7. Whole body imaging

Three mice from each treatment were left intact for analysis by whole body fluorescent imaging using the iBox Scientia Small Animal Imaging System (UVP) throughout the course of the study. Mice were imaged at the same time points ($T = 1H$, 3H, 5H, 24H, 3D, 5D, 7D, 14D, 30D, and 60D post-mortem) using the parameters: 75 tray height, 580–630 nm RFP filter, intensity of 5, and a two second exposure.

3. Results

Whole body fluorescent imaging and culture-based methods of tracking *S. aureus* KUB7 and *C. perfringens* showed transmigration during murine decomposition. Whole body fluorescent imaging showed *S. aureus* KUB7 nasal colonization 1H post sacrifice in the surface sterilized and non-surface sterilized mice (Fig. 1, panels A and B). Imaging showed evidence of increased *S. aureus* KUB7 transmigration occurring in the non-surface sterilized mice over decomposition time. *S. aureus* KUB7 was at the highest detectable

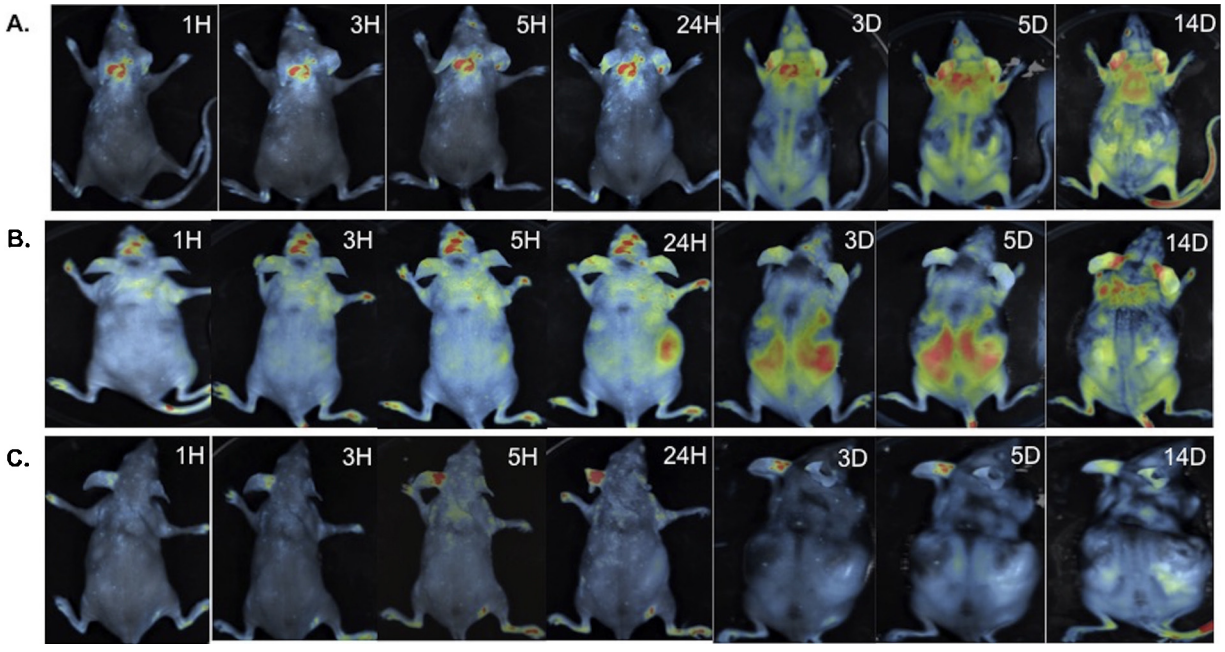

Fig. 1. Whole body imaging using iBox Scientia (UVP) detecting *Staphylococcus aureus* KUB7 translocation in infected, surface sterilized (A), infected, non-surface sterilized (B) and uninfected, control mice (C) 1H, 3H, 5H, 24H, 3D, 5D, and 14D post mortem. The intensity of fluorescence is based on a scale from blue being the lowest and red being the highest.

concentrations within the nasopharyngeal area among surface sterilized mice up to 24H, but was detected throughout the body among non-surface sterilized mice during this timeframe. Increased visible evidence of transmigration was found from 3D to 14D in both sample sets. Imaging 30D post sacrifice showed elevated autofluorescence of control mice that continued (though with decreasing intensity) throughout the remaining time points of the 60D study (data not shown). Autofluorescence was likely due to breakdown of blood over time that became detectable within the fluorescence spectra of RFP [16]. Autofluorescence of control mice prevented identification of *S. aureus* KUB7 among treatment groups using whole-body imaging from samples collected 30D and 60D post sacrifice.

S. aureus KUB7 was isolated from all analyzed organ swabs from surface sterilized mice 1H post sacrifice and from all analyzed organ swabs from the non-surface sterilized mice except for the liver (Fig. 2). Swabs from liver, stomach, intestine, and skin remained positive 3H post sacrifice and up to 14D for both surface and non-surface sterilized mice, except for negative intestine samples from surface sterilized mice at the 7D time point. Remaining organs showed undulating positivity from 3D to 14D post sacrifice (Fig. 2) in both treatment groups. In comparison to surface sterilized mice, *S. aureus* KUB7 was detected in more of the analyzed organs from non-surface sterilized mice from the 3H, 24H, and 7D time points (6, 7, and 8 positive organs as opposed to 5, 5, and 5 positive organs from surface-sterilized mice at the respective time points). Surface sterilized mice had more organs positive than non-surface sterilized mice organs 1H and 5D post sacrifice (8 organs *versus* 7 respectively at both time points). Both treatment groups showed six positive organs 5H, and eight organs 14D post sacrifice. All analyzed organs, however, were negative for 30D and 60D post sacrifice time points (Fig. 3).

The inability of *C. perfringens* WAL 14572 to withstand oxygen exposure was confirmed by culturing a 2.8×10^8 CFU/mL *C. perfringens* inoculum following aerobic exposure. The culture was anaerobically incubated and did not yield colonies. However, growth of anaerobic bacteria including non-specific clostridium was measured on reinforced clostridial medium and showed varying numbers of anaerobic bacteria in liver, lung, spleen, heart, and intestine samples from the 1H to 24H time points among both treatment groups that reached and remained at maximum countable limits 5D to 14D. Isolates were also recovered from these

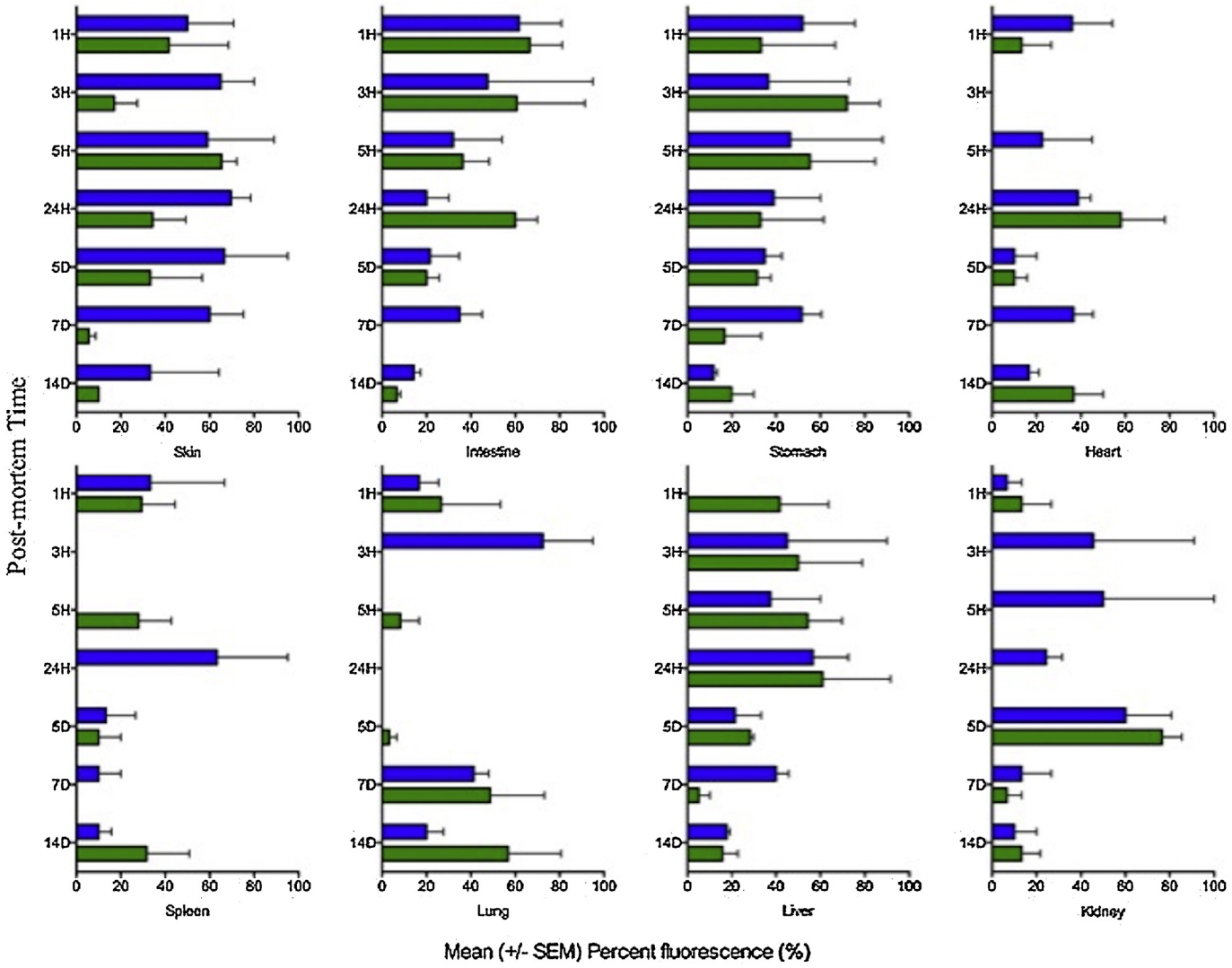

Fig. 2. Mean percentage of (± Standard Error of the Mean, SEM) *Staphylococcus aureus* KUB7 colonies isolated from mouse organs over time. Kidney, liver, lung, spleen, heart, stomach, intestines, and skin samples were analyzed for *S. aureus* KUB7 isolated 1H to 60D post sacrifice. Blue bars represent mean percent of fluorescent colonies among organs from non-surface sterilized mice. Green bars represent mean percent of fluorescent colonies among organs from surface sterilized mice. (For interpretation of the references to color in this figure legend, the reader is referred to the web version of this article.)

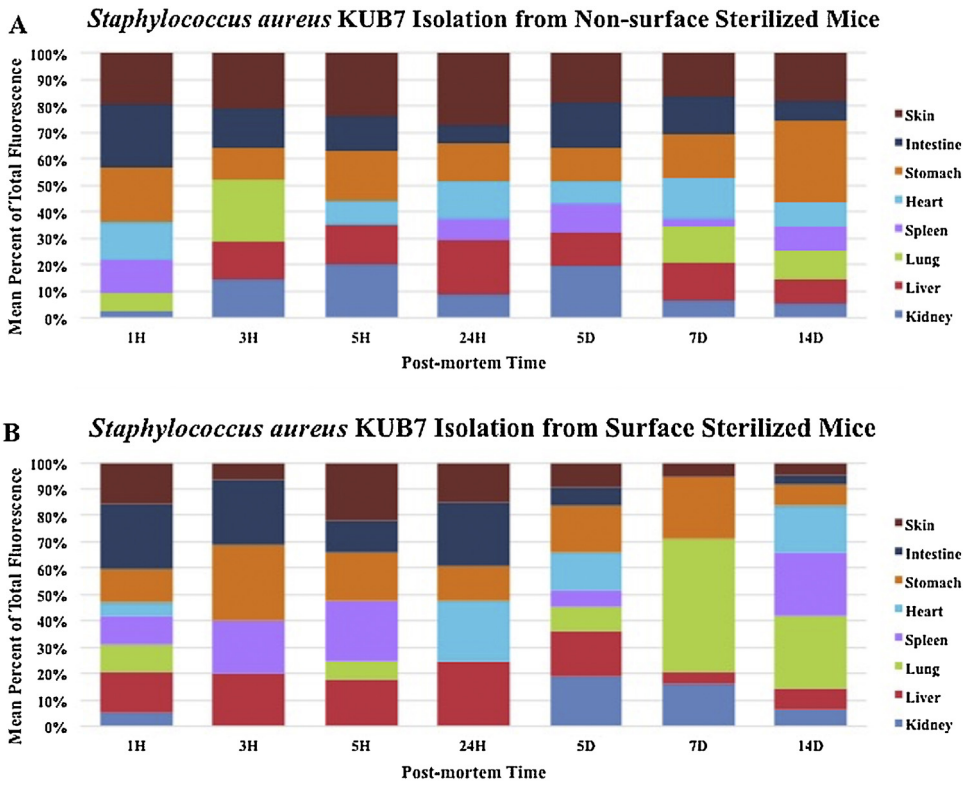

Fig. 3. *Staphylococcus aureus* KUB7 isolation from (A) non-surface sterilized mice and (B) surface sterilized mice by culture on MSA detected by plate count and fluorescence confirmation using fluorescent microscopy. Triplicates were averaged for mean fluorescence associated with each organ then compared to the total fluorescence present across all organs at the different post-mortem times up to 14D. The 30D and 60D time points were not included as *S. aureus* KUB7 was not detected at those time points.

samples at 30 and 60D, though differences were found in bacterial counts between sampled organs and treatment groups (Fig. 4). Kidney samples from both treatment groups showed undulating positivity throughout the study where surface sterilized mice kidney samples increased to reach maximum countable bacterial numbers at 5D and 7D, but decreased 14D, 30D, and 60D. Kidney samples from non-surface sterilized mice increased to reach maximum countable bacterial numbers at 7D and 14D, but decreased at 30D and 60D. Anaerobic bacteria were differentially isolated from skin samples among treatment groups 1H to 24H post sacrifice, but reached maximum countable numbers 5D to 7D, where they subsequently showed differences in bacterial isolates from both treatment groups at 14D, 30D and 60D (Fig. 4).

4. Discussion and conclusions

We have expanded current studies of post-mortem microbial transmigration by providing data of intentionally inoculated bacteria transmigration dynamics following host death. Ante-mortem infection with *S. aureus* KUB7 and *C. perfringens* WAL 14572 allowed controlled and specific tracking of model commensal organisms through the nasal tract using *in vivo* and *in vitro* imaging and culture methods (Figs. 1–4). As expected for this study, a strict anaerobe, *C. perfringens* WAL 14572, was not viable following exposure to aerobic conditions. However, results showed *S. aureus* KUB7 was infected in the nasal tract where transmigration was detected at the earliest time point following host death, reaching its highest concentrations by culture on 5D and 7D for surface sterilized and non-surface sterilized mice, respectively. Non-surface sterilized mice showed a wider distribution of *S. aureus* KUB7 presence in organs over time both from culture and from whole body imaging. Additionally, *S. aureus* KUB7 was detected during the majority of decomposition among organs, such as the stomach and intestines, which are normally heavily colonized in the living host; whereas previously sterile organs, such as the kidney, liver, spleen, and heart, showed undulating positivity over time. It is possible that *S. aureus* KUB7 was ingested soon following infection leading to instant colonization; however, it is also possible that ante-mortem indigenous microbes contribute to *S. aureus* KUB7 colonization post-mortem, perhaps through providing nutrients or aiding in elimination of toxins resulting from decomposition.

Kidney, lung, spleen, and heart showed undulating positivity 3D to 7D for both infection groups. For instance, *S. aureus* KUB7 was detected in kidneys 1H post sacrifice from both treatment groups, was not detected from kidneys of surface sterilized mice 3H, 5H, and 24H post sacrifice, but was detected again 5D through 14D. Heimesaat et al. [4] showed similar findings from their intestinal transmigration study [4]. Their data showed the total bacterial load in the small intestines increased 12 and 24H post sacrifice due to high levels of enterobacteria and lactobacilli. They noticed a decline in total bacterial load 15 and 30 min post-mortem due to significant decreases in enterobacteria, enterococci, bifidobacteria, and *Clostridium* spp. [4] with a subsequent increase in the bacterial groups reaching maximum levels at the end of the study. The authors speculated that the undulating pattern might be associated with physiological changes in the intestinal intraluminal milieu during temporal decomposition stages [4]. The authors also found intestinal tissue destruction characterized by an increase in apoptotic cells and neutrophils within 3H post-mortem, with T- and B-lymphocytes and regulatory T-cells decreasing between 3 and 12H post-mortem that could compromises the replication of the intestinal bacteria at specific time points. Though more data needs to be gathered, our data support initial interpretations of Heimesaat et al. [4]. All cadavers were held at constant temperature, however body temperature and decomposition

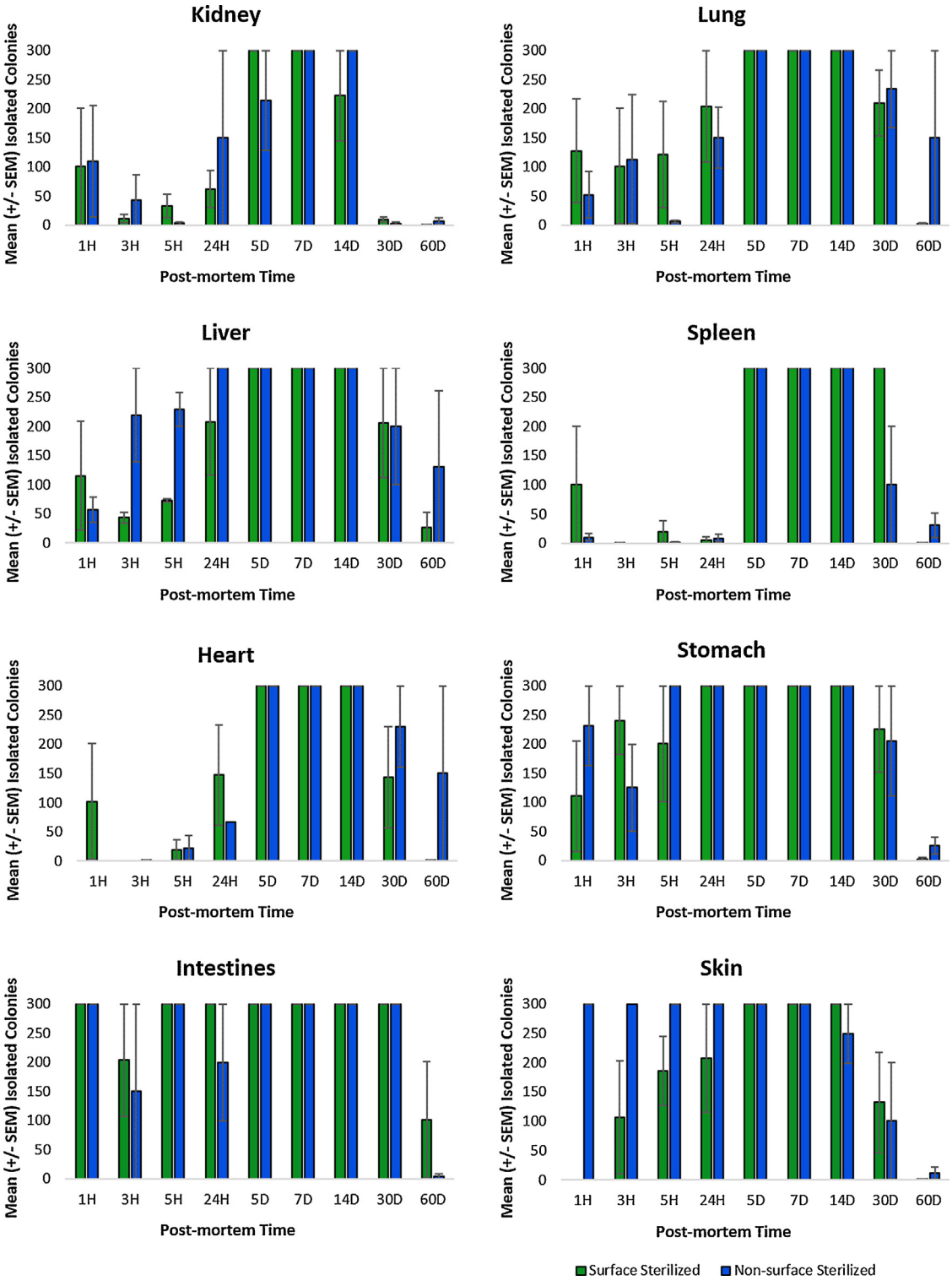

Fig. 4. Mean (± Standard Error of the Mean, SEM) isolated anaerobic colonies among organs over time. Kidney, liver, lung, spleen, heart, intestine, stomach, and skin swabs from non-surface and surface sterilized mice were analyzed by culture on reinforced clostridial medium (RCM) incubated anaerobically. Blue bars represent samples obtained from non-surface sterilized mice and green bars represent samples from surface sterilized mice. Colony counts greater than or equal to 300 on a single plate were considered to have maximum countable colonies and no error bars were expected.

stages were evident at discrete time points potentially explaining some of the observed patterns of bacterial culture and transmigration to specific organs (data not shown).

Anaerobic organisms were isolated at every time point, and increased in concentration over time, especially for organs considered to be sterile ante-mortem, such as the kidney, liver, and spleen, and also for skin. However, there was a decrease in these organisms by the end of the study. Replicate variability was observed in some of the sample from both treatment groups, possibly a reflection of the sample size ($N = 3$) in each group. Additionally, specific anaerobic species were not identified here that could influence successional colonization events over time.

Furthermore, our results mirror those found from other animal surrogate studies that showed a shift from aerobic to anaerobic microbial taxa through progressive successional decomposition stages [3,8,9,17]. Studies are currently underway using molecular methods to quantify microbial response from intentionally infected bacteria and identify associated microbial consortia from anaerobic organs following host decomposition in order to identify significant differences between anatomical locations and oxygen conditions, which may be used as reliable indicators for time since death.

As cadavers decompose, the environment inside the body undergoes rapid changes such as oxygen availability, pH, and nutrient availability [1,17]. It is known that microbial communities that were a part of the normal bacterial flora of the once living host play a significant role in decomposition, and that these communities are highly dynamic [1,8,18]. These communities thrive in a living host by utilizing the nutrients and surface areas provided by the host, and are usually kept to a specific niche by the living host's immune system. Following host death, the body becomes a large nutrient source and niche for specific microbial communities that begin to transmigrate to previously sterile locations in the body due to the gradual loss of a functional immune system that can no longer travel throughout the body by blood circulation [1]. Changes in this environment, such as oxygen availability, and increase in toxicity also likely select for microbial species that can survive the shifting environment by regulating their gene expression and products to accommodate their survival needs as their environment changes. Bacteria respond to stress and dynamic environmental conditions by modulating gene expression that controls the cell's structure and function, [19,20], and an extreme stress will force some microbes to dormancy or death [21]. Competition and dispersal among microbial communities also occurs when resources become limited [22,23]. This ecosystem shift causes community instability until dominant organisms outcompete those that are less tolerant or resilient [22]. It is likely that *S. aureus* KUB7 modulated gene expression to adapt to physiological changes associated with each anatomical location. Additionally, other members of the microbial consortium likely contributed to presence or absence of *S. aureus* both temporally and spatially.

In addition to the data presented in this study, we are currently using additional molecular methods, data not presented, to survey the entire microbial consortium associated with each organ in order to obtain information on interacting microbial taxa during dispersal associated with physiological conditions of decomposition events. A comprehensive understanding of the impact of anatomical location on microbial transmigration and subsequent microbial mechanisms of host decomposition is key in determining colonization routes correlating to the changes in decomposition process across the post-mortem interval. Identifying consistent post-mortem temporal shifts of a biological indicator, such as a microbial taxon or community transmigration, may prove to be useful in future forensic applications by providing more specific PMI range estimates. These data are an additional step to identify post-mortem microbial movement or metabolic signatures for applications in the potential use to improve quantifiable, precise measurements of PMI estimates in forensic science.

Acknowledgments

We would like to thank the following: Mississippi State University, Mississippi State University College of Veterinary Medicine, Michigan State University, University of Michigan, and the Wayne County Medical Examiner's Office. Thank you to Dr. Jean Feugang for training and access to the iBox imaging system. Funding was provided by the National Institute of Justice (2014-DN-BX-K008) and Mississippi State University. Opinions or points of view expressed on represent a consensus of the authors and do not necessarily represent the official position or policies of the U.S. Department of Justice.

References

[1] R.C. Janaway, S.L. Percival, A.S. Wilson, Decomposition of human remains, in: S.L. Percival (Ed.), Microbiology and Aging: Clinical Manifestations, Humana Press, 2009.
[2] A.T. Schafer, Colour measurements of pallor mortis, Int. J. Legal Med. 113 (2) (2000) 81–83.
[3] J.R. Melvin Jr., L.S. Cronholm, L.R. Simson Jr., A.M. Isaacs, Bacterial transmigration as an indicator of time of death, J. Forensic Sci. 29 (2) (1984) 412–417.
[4] M.M. Heimesaat, S. Boelke, A. Fischer, L.M. Haag, C. Loddenkemper, A.A. Kuhl, et al., Comprehensive postmortem analyses of intestinal microbiota changes and bacterial translocation in human flora associated mice, PLoS ONE 7 (7) (2012) e40758, http://dx.doi.org/10.1371/journal.pone.0040758.
[5] H.F. Wertheim, D.C. Melles, M.C. Vos, W. van Leeuwen, A. van Belkum, H.A. Verbrugh, et al., The role of nasal carriage in *Staphylococcus aureus* infections, Lancet Infect. Dis. 5 (12) (2005) 751–762, http://dx.doi.org/10.1016/S1473-3099(05)70295-4.
[6] F.A. Uzal, B.A. McClane, J.K. Cheung, J. Theoret, J.P. Garcia, R.J. Moore, et al., Animal models to study the pathogenesis of human and animal *Clostridium perfringens* infections, Vet. Microbiol. 179 (1–2) (2015) 23–33, http://dx.doi.org/10.1016/j.vetmic.2015.02.013.
[7] M. Nagahama, S. Ochi, M. Oda, K. Miyamoto, M. Takehara, K. Kobayashi, Recent insights into *Clostridium perfringens* beta-toxin, Toxins (Basel) 7 (2) (2015) 396–406, http://dx.doi.org/10.3390/toxins7020396.
[8] J.L. Pechal, T.L. Crippen, M.E. Benbow, A.M. Tarone, S. Dowd, J.K. Tomberlin, The potential use of bacterial community succession in forensics as described by high throughput metagenomic sequencing, Int. J. Legal Med. 128 (1) (2014) 193–205, http://dx.doi.org/10.1007/s00414-013-0872-1.
[9] J.L. Pechal, T.L. Crippen, A.M. Tarone, A.J. Lewis, J.K. Tomberlin, M.E. Benbow, Microbial community functional change during vertebrate carrion decomposition, PLoS ONE 8 (11) (2013) e79035, http://dx.doi.org/10.1371/journal.pone.0079035.
[10] J.L. Bose, P.D. Fey, K.W. Bayles, Genetic tools to enhance the study of gene function and regulation in *Staphylococcus aureus*, Appl. Environ. Microbiol. 79 (7) (2013) 2218–2224, http://dx.doi.org/10.1128/AEM. 00136-13.
[11] Y.Y. Pang, J. Schwartz, M. Thoendel, L.W. Ackermann, A.R. Horswill, W.M. Nauseef, agr-Dependent interactions of *Staphylococcus aureus* USA300 with human polymorphonuclear neutrophils, J. Innate Immun. 2 (6) (2010) 546–559, http://dx.doi.org/10.1159/000319855.
[12] J. Chen, P. Yoong, G. Ram, V.J. Torres, R.P. Novick, Single-copy vectors for integration at the SaPI1 attachment site for *Staphylococcus aureus*, Plasmid 76C (2014) 1–7, http://dx.doi.org/10.1016/j.plasmid.2014.08.001.
[13] K.L. Krausz, J.L. Bose, Bacteriophage transduction in *Staphylococcus aureus*: broth-based method, Methods Mol. Biol. 1373 (2016) 63–68, http://dx.doi.org/10.1007/7651_2014_185.
[14] I.R. Monk, I.M. Shah, M. Xu, M.W. Tan, T.J. Foster, Transforming the untransformable: application of direct transformation to manipulate genetically *Staphylococcus aureus* and *Staphylococcus epidermidis*, MBio 3 (2) (2012), http://dx.doi.org/10.1128/mBio.00277-11.
[15] B.R. Boles, M. Thoendel, A.J. Roth, A.R. Horswill, Identification of genes involved in polysaccharide-independent *Staphylococcus aureus* biofilm formation, PLoS ONE 5 (4) (2010) e10146, http://dx.doi.org/10.1371/journal.pone.0010146.
[16] T.B. Feldman MAY, A.E. Dontsov, M.A. Ostrovsky, Fluorescence emission and excitation spectra of fluorophores of lipofuscin granules isolated from retinal pigment epithelium of human cadaver eyes, Russ. Chem. Bull. 59 (1) (2010) 276–283.
[17] J.L. Metcalf, L. Wegener Parfrey, A. Gonzalez, C.L. Lauber, D. Knights, G. Ackermann, et al., A microbial clock provides an accurate estimate of the postmortem interval in a mouse model system, Elife 2 (2013) e01104, http://dx.doi.org/10.7554/eLife.01104.
[18] G.L.R. Payen, M. Gueux, N. Lery, Body putrefaction in "air tight" burials. Microbiologic findings and environment, Acta Med. Leg. Soc. 38 (1988) 153–163.
[19] P.D. Cotter, C. Hill, Surviving the acid test: responses of gram-positive bacteria to low pH, Microbiol. Mol. Biol. Rev. 67 (3) (2003) 429–453.
[20] E.Z. Ron, Editorial: an update on the bacterial stress response, Res. Microbiol. 160 (4) (2009) 243–244, http://dx.doi.org/10.1016/j.resmic.2009.04.001.
[21] J. Schimel, T.C. Balser, M. Wallenstein, Microbial stress–response physiology and its implications for ecosystem function, Ecology 88 (6) (2007) 1386–1394.
[22] D.M. Cornforth, K.R. Foster, Competition sensing: the social side of bacterial stress responses, Nat. Rev. Microbiol. 11 (4) (2013) 285–293.
[23] K.J. Boor, Bacterial stress responses: what doesn't kill them can make then stronger, PLoS Biol. 4 (1) (2006) e23.